AJNR

Subtraction CT angiography with controlled-orbit helical scanning for detection of intracranial aneurysms.

S Imakita, Y Onishi, T Hashimoto, S Motosugi, S Kuribayashi, M Takamiya, N Hashimoto, T Yamaguchi and T Sawada

AJNR Am J Neuroradiol 1998, 19 (2) 291-295
http://www.ajnr.org/content/19/2/291

AJNR Am J Neuroradiol 19:291–295, February 1998

Subtraction CT Angiography with Controlled-Orbit Helical Scanning for Detection of Intracranial Aneurysms

Satoshi Imakita, Yoshitaka Onishi, Tokihiro Hashimoto, Shin Motosugi, Sachio Kuribayashi, Makoto Takamiya, Nobuo Hashimoto, Takenori Yamaguchi, and Tohru Sawada

PURPOSE: **Our goal was to evaluate the utility of subtraction three-dimensional CT angiography for the detection of intracranial aneurysms.**

METHODS: **Thirty-six patients with intracranial aneurysms were examined using newly devised controlled-orbit helical scanning and conventional angiography. Three-dimensional CT angiograms and subtraction 3-D CT angiograms were compared with conventional angiograms for their characterization of intracranial aneurysms.**

RESULTS: **Fifty aneurysms were depicted on conventional angiograms, of which 48 (96%) were seen on the 3-D CT angiograms. Three-dimensional CT angiography was superior or equivalent to conventional angiography for depicting the shape, direction, and location of 33 (66%) of 50 aneurysms; however, it was often less useful than conventional angiography in delineating intracranial aneurysms adjacent to bone. Subtraction 3-D CT angiograms were obtained in 32 patients with a total of 46 aneurysms (in four cases, aneurysms were not depicted owing to excessive motion artifacts), and were superior or equivalent to conventional angiograms in all 46 cases.**

CONCLUSIONS: **Subtraction 3-D CT angiography with the use of controlled-orbit helical scanning is effective in the detection of intracranial aneurysms.**

Several authors have reported the usefulness of three-dimensional computed tomographic (CT) angiography with rapid sequence scanning in the diagnosis of intracranial aneurysms (1–4). However, because the data from these CT studies were not obtained in a continuous volume, 3-D CT angiography was not always able to depict small lesions. Helical CT scanning does obtain data in a continuous volume; therefore, 3-D CT angiography with helical scanning may be a potentially valuable tool (5–9). Three-dimensional CT angiography is less useful than conventional angiography in the detection of intracranial aneurysms adjacent to bone. If subtraction 3-D CT angiography can be obtained, it may be useful for establishing the presence of these aneurysms.

The purpose of this study was to evaluate the usefulness of subtraction 3-D CT angiography in the detection of intracranial aneurysms.

Received March 18, 1997; accepted after revision August 20.

Presented at the annual meeting of the American Society of Neuroradiology, Seattle, Wash, June 1996.

From the Departments of Radiology (S.I., Y.O. T.H., S.M., S.K., M.T.), Neurosurgery (N.H.), and Internal Medicine (Cerebrovascular Division) (T.Y., T.S.), National Cardiovascular Center, Suita-city, Osaka, Japan.

Address reprint requests to Satoshi Imakita, MD, Department of Radiology, National Cardiovascular Center, 5–7–1 Fujishiro-dai, Suita-city, Osaka 565 Japan.

Methods

Thirty-six patients (20 women and 16 men, 29 to 78 years old) were studied with 3-D CT angiography, subtraction 3-D CT angiography with helical scanning, and conventional angiography, including digital subtraction angiography (Table). Informed consent for helical CT and conventional angiography was obtained from all patients. Patients' heads were tightly fixed to prevent motion artifacts and to obtain exactly subtracted images during helical scanning. The gantry of the CT scanner was not tilted.

Helical CT scanning for 3-D CT angiography and subtraction 3-D CT angiography was performed using the following parameters: 120 kV, 150 mA, scan time of 1 second per rotation, 1-mm collimation, and a table speed of 1 mm/s during 52 to 57 seconds of continuous exposure. The data for 3-D CT angiography and subtraction 3-D CT angiography were obtained with the use of our newly devised controlled-orbit helical scanning method, which synchronized the table movement and X-ray tube rotation to identify the X-ray tube orbit for the repetition of helical scanning. Immediately after the data from the unenhanced helical scan were obtained, an injection of contrast medium was started. The contrast medium (iohexol 350) was injected via an antecubital vein biphasically for 30 seconds at the rate of 1.0 to 1.5 mL/s, followed immediately by a rate of 0.7 to 1.0 mL/s. Total volume was 1.2 to 1.5 mL/kg of body weight (60 to 90 mL). Acquisition of data from the enhanced helical scan was begun 40 to 45 seconds after contrast

Comparison of the detectability of intracranial aneurysms (3-D CT angiography and subtraction 3-D CT angiography versus conventional angiography)

Patient	Age, y/Sex	Site of Aneurysm	Detection of Aneurysm	
1	32/F	L ICA-PCA	CT > AG	SB > AG
		L ICA-AChA	CT > AG	SB > AG
2	57/F	L ICA-PCA	CT = AG	SB = AG
3	58/F	L ICA-PCA	CT = AG	SB = AG
4	60/M	L ICA-PCA	CT < AG	SB = AG
		L IC-AChA	CT = AG	SB = AG
5	65/M	R ICA-PCA	CT < AG	SB = AG
6	66/M	L ICA-PCA	CT < AG	SB = AG
		BA	CT > AG	SB > AG
7	67/F	R ICA-PCA	CT = AG	SB = AG
		L ICA-PCA	CT = AG	SB = AG
		R MCA(bif)	CT > AG	SB > AG
		BA top	CT > AG	SB > AG
8	67/M	R ICA-PCA	CT = AG	SB = AG
9	70/F	L ICA-PCA	CT < AG	SB = AG
10	70/M	R ICA-PCA*	CT < AG	SB = AG
11	74/M	R ICA-PCA	CT > AG	SB > AG
12	29/F	L ICA-Oph	CT < AG	SB > AG
13	43/F	R ICA-Oph	CT < AG	...
14	47/M	L ICA-Oph	CT < AG	...
15	58/F	R ICA-Oph	CT < AG	SB = AG
		L ICA-Oph	CT < AG	SB = AG
16	62/F	R ICA-Oph	CT < AG	SB > AG
		R ACA	CT = AG	SB = AG
		BA top	CT > AG	SB > AG
17	75/F	R ICA-Oph	CT < AG	SB = AG
18	71/F	R ICA-AChA	CT < AG	SB = AG
		L ICA-AChA*	CT < AG	SB = AG
		R MCA(bif)	CT > AG	SB > AG
19	33/M	R ICA(C1)	CT > AG	SB > AG
20	55/M	R ICA(C1)	CT < AG	SB > AG
21	61/F	L ICA(cav)	CT < AG	...
22	76/F	R ICA(cav)	CT < AG	...
23	39/M	R MCA(M1)	CT = AG	SB = AG
		L MCA(M1)	CT > AG	SB > AG
24	54/M	R MCA(bif)	CT > AG	SB > AG
25	68/F	L MCA(M1)	CT > AG	SB > AG
26	74/F	R MCA(bif)	CT > AG	SB > AG
27	74/F	R MCA(bif)	CT > AG	SB > AG
		AComA	CT > AG	SB > AG
28	75/F	R MCA(bif)	CT > AG	SB > AG
		BA top	CT > AG	SB > AG
29	56/M	AComA	CT > AG	SB > AG
30	78/M	AComA	CT > AG	SB > AG
31	56/F	BA top	CT > AG	SB > AG
32	70/M	BA top	CT > AG	SB > AG
33	75/F	BA top	CT > AG	SB > AG
34	42/M	R VA	CT > AG	SB > AG
35	48/F	R VA	CT > AG	SB > AG
36	55/M	R VA	CT > AG	SB > AG

* Invisible on 3-D CT angiograms.

Note.—CT indicates 3-D CT angiography; SB, subtraction 3-D CT angiography; AG, conventional angiography; ICA, internal carotid artery; ACA, anterior cerebral artery; MCA, middle cerebral artery; PCA, posterior communicating artery; AChA, anterior choroidal artery; Oph, ophthalmic artery; AComA, anterior communicating artery; BA, basilar artery; VA, vertebral artery; bif, bifurcation; and cav, cavernous portion.

injection was initiated. The 1-mm sections were reconstructed at a 0.5-mm pitch using a 360° interpolation method. Reconstructed images were transferred to X link 50 or X tension. Three-dimensional reconstruction of these axial sections was performed by using a surface-rendering method with X link 50 or a volume-rendering method with X tension. The matrix size was 512 × 512. With X link 50, the lower threshold level varied from 80 to 100 Hounsfield units (HU) among patients, and a fixed upper threshold of 4000 HU was used. Three-dimensional CT angiograms were black and white with X link 50; with X tension, the 3-D CT angiograms were reconstructed in color-coded shaded-surface display: the vasculature showing 80 to 280 HU was orange and the calcification and bone showing over 280 HU were white.

Subtraction 3-D CT angiograms were reconstructed from the axial subtracted images, which were obtained from enhanced and unenhanced helical data by the same reconstruction method as with 3-D CT angiograms. In several cases, the surrounding veins and cavernous sinus were manually excluded on the axial subtracted images before 3-D reconstruction to enhance visibility of the aneurysms. The 3-D CT angiograms and subtraction 3-D CT angiograms were interpreted by three radiologists without knowledge of the findings on conventional angiograms; the visibility of aneurysms on 3-D CT angiograms and subtraction 3-D CT angiograms was compared with that on conventional angiograms.

Results

A total of 50 aneurysms were depicted on conventional angiograms (Table). There were nine aneurysms of the middle cerebral artery (MCA), one of the anterior cerebral artery (ACA), three of the anterior communicating artery (AComA), seven of the basilar artery, three of the vertebral artery, 12 of the internal carotid artery–posterior communicating artery (ICA-PCA), seven of the ICA-ophthalmic artery, four of the ICA-anterior choroidal artery, and four other aneurysms of the ICA (two of the C1 portion and two of the cavernous portion). Forty-eight (96%) of the 50 aneurysms were depicted by 3-D CT angiography. Three-dimensional CT angiography was superior or equivalent to conventional angiography in depicting the shape, direction, and location of 33 (66%) of the 50 aneurysms. Three-dimensional CT angiography clearly depicted wall calcification. The aneurysms were classified into either the superior group (3-D CT angiography better than or equal to conventional angiography) or the inferior group (3-D CT angiography worse than conventional angiography).

Superior Group (3-D CT Angiography Better than or Equal to Conventional Angiography)

Nine MCA aneurysms, one ACA aneurysm, three AComA aneurysms, seven basilar artery aneurysms, and three vertebral artery aneurysms were included in this group. These 23 aneurysms were clearly delineated on 3-D CT angiograms. Ten (37%) of 27 ICA aneurysms were also included in this group. These consisted of seven ICA-PCA aneurysms, two ICA-anterior choroidal artery aneurysms, and one ICA (C1 portion) aneurysm. The 10 ICA aneurysms were clearly delineated on 3-D CT angiograms (Fig 1).

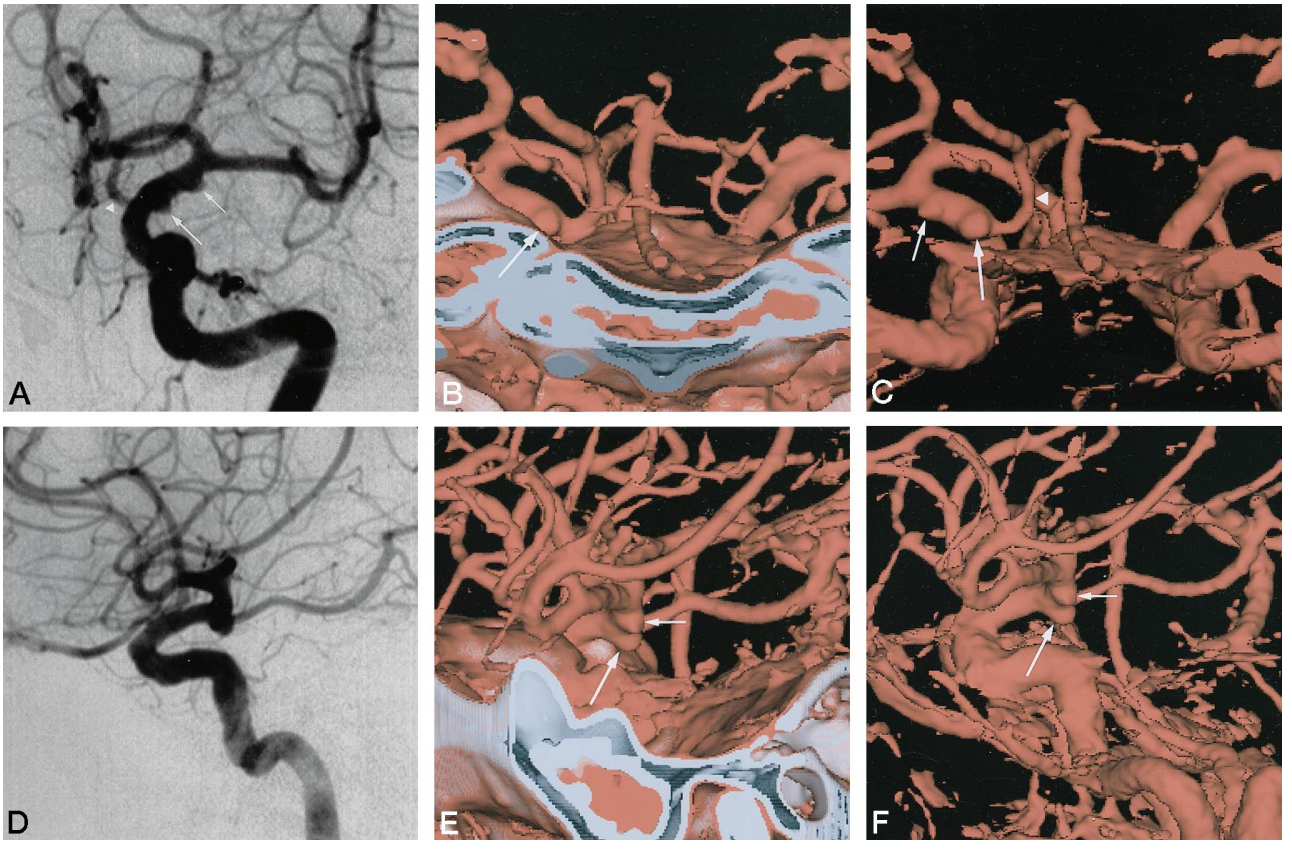

FIG 1. Case 1: Patient with aneurysms of the left ICA-PCA and left ICA-anterior choroidal artery.

A, Left carotid angiogram (anteroposterior view) shows aneurysms of the ICA-PCA (*long arrow*), PCA (*arrowhead*), and ICA-anterior choroidal artery (*short arrow*).

B, Three-dimensional CT angiogram (posterior view) shows ICA-PCA aneurysm (*arrow*). ICA-anterior choroidal artery aneurysm is not depicted clearly.

C, Subtraction 3-D CT angiogram (posterior view) clearly shows ICA-PCA aneurysm (*long arrow*) at the left ICA just distal to the orifice of the PCA (*arrowhead*), and an ICA-anterior choroidal artery aneurysm (*short arrow*).

D, On left carotid angiogram (lateral view), the two aneurysms cannot be differentiated.

E, Three-dimensional CT angiogram (left lateral view) clearly shows ICA-PCA aneurysm (*long arrow*) and ICA-anterior choroidal artery aneurysm (*short arrow*).

F, Subtraction 3-D CT angiogram (left lateral view) clearly shows the two aneurysms (*arrows*) and the entire left ICA. This patient underwent clipping of a left ICA-PCA aneurysm and coating of a left ICA-anterior choroidal artery aneurysm.

Inferior Group (3-D CT Angiography Worse than Conventional Angiography)

Seventeen (63%) of the 27 ICA aneurysms were included in this group. Fifteen (56%) were depicted on 3-D CT angiograms but could not be clearly distinguished from adjacent bone; these included four ICA-PCA aneurysms, one ICA-anterior choroidal artery aneurysm, seven ICA-ophthalmic artery aneurysms, one ICA (C1 portion) aneurysm, and two ICA (cavernous portion) aneurysms. Two (7%) of 27 ICA aneurysms could not be seen on 3-D CT angiograms; these included one ICA-PCA aneurysm and one ICA-anterior choroidal artery aneurysm (Figs 2 and 3).

Subtraction 3-D CT angiograms were obtained in 32 patients with a total of 46 aneurysms. Subtraction 3-D CT angiograms could not be obtained in four patients (with a total of four ICA aneurysms) owing to excessive motion artifacts. In all 23 aneurysms of the MCA, ACA, AComA, basilar, and vertebral arteries, subtraction 3-D CT angiography was superior or equivalent to conventional angiography for depicting their shape, direction, and location. In the remaining 23 ICA aneurysms, consisting of 10 aneurysms belonging to the superior group and 13 belonging to the inferior group, subtraction 3-D CT angiography was superior or equivalent to conventional angiography (Figs 2–4).

In a patient who underwent clipping of a left MCA aneurysm (case 18), 3-D CT angiograms did not show the left ICA-anterior choroidal artery aneurysm and vessels adjacent to the clip because of the presence of metal artifacts. However, these artifacts could be removed on the subtraction 3-D CT angiograms, enabling the aneurysm and surrounding vessels to be seen on subtraction 3-D CT angiograms (Fig 3).

Discussion

Three-dimensional CT angiography can depict intracranial aneurysms from multiple directions, as well as the surrounding vasculature and bone. Therefore, the location of aneurysms should be easier to discern

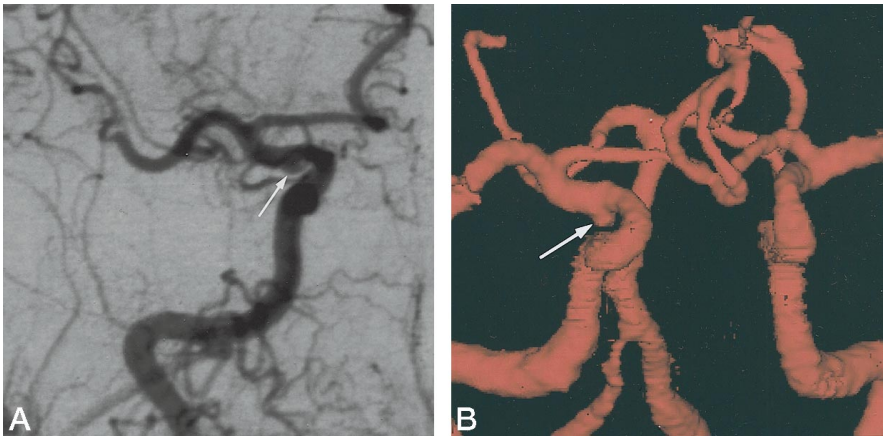

FIG 2. Case 10: Patient with an aneurysm of the right ICA-PCA.

A, Right carotid angiogram (anteroposterior view) shows ICA-PCA aneurysm (*arrow*) directed downward.

B, Subtraction 3-D CT angiogram (anterior view) clearly shows ICA-PCA aneurysm (*arrow*). This patient refused an operation.

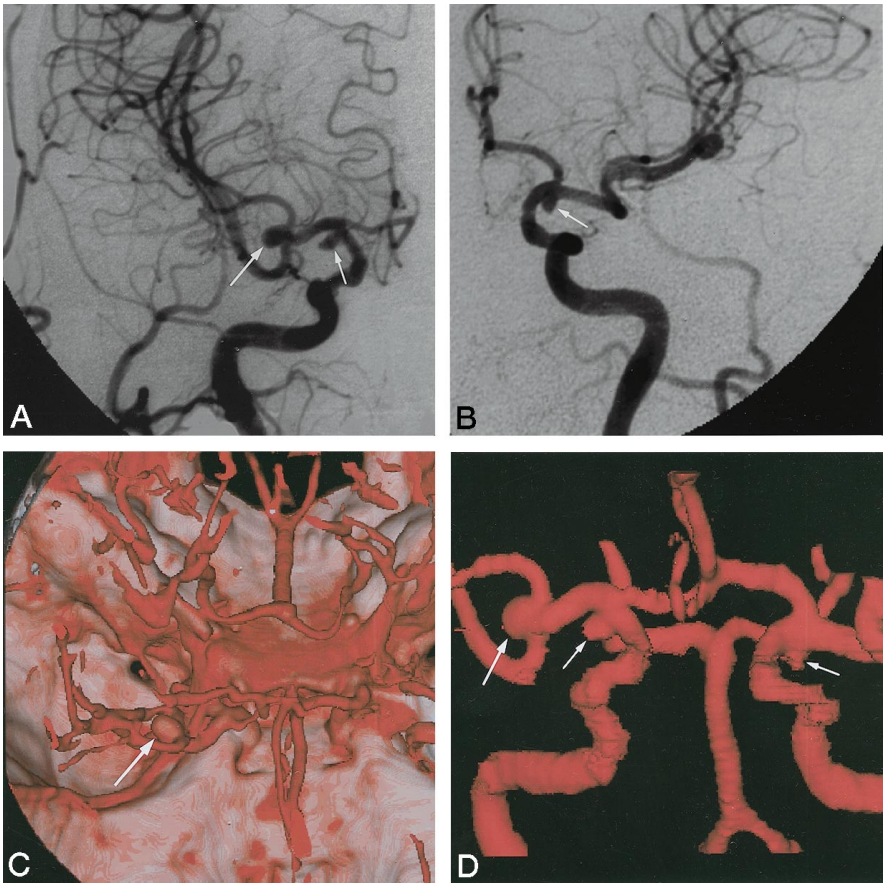

FIG 3. Case 18: Patient with an aneurysm of the right MCA bifurcation and bilateral aneurysms of the ICA-anterior choroidal artery who had prior clipping of an aneurysm of the left MCA bifurcation.

A, Right carotid angiogram (anteroposterior view) shows aneurysms of the MCA bifurcation (*long arrow*) and the ICA-anterior choroidal artery (*short arrow*).

B, Left carotid angiogram (anteroposterior view) shows ICA-anterior choroidal artery aneurysm (*arrow*).

C, Three-dimensional CT angiogram (superior view) shows right MCA bifurcation aneurysm (*arrow*). Right ICA-anterior choroidal artery aneurysm cannot be clearly distinguished from surrounding structures. Left ICA-anterior choroidal artery aneurysm is not depicted. Left M1 segment is not seen owing to artifacts related to the clip.

D, Subtraction 3D-CT angiogram (anterior view) clearly shows right MCA bifurcation aneurysm (*long arrow*) and bilateral ICA-anterior choroidal artery aneurysms (*short arrows*).

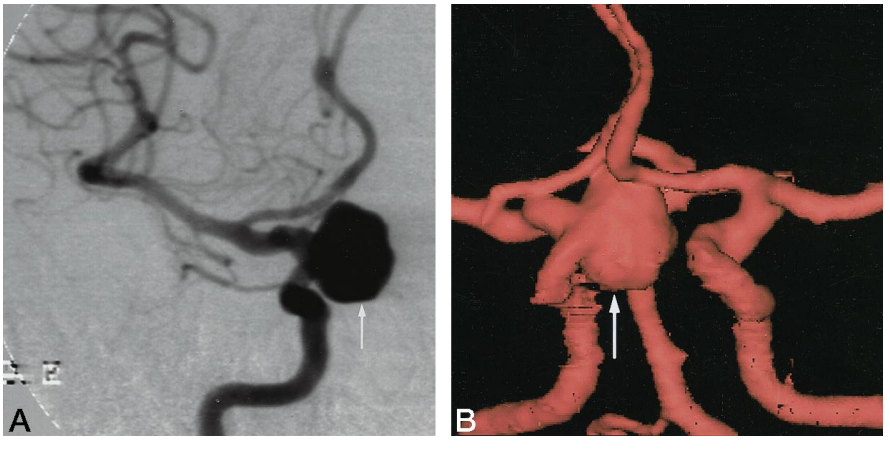

FIG 4. Case 16: Patient with an aneurysm of the right ICA-ophthalmic artery.

A, Right carotid angiogram (left anterior oblique view) shows a large ICA-ophthalmic artery aneurysm (*arrow*).

B, Subtraction 3-D CT angiogram (left anterior oblique view) shows the ICA-ophthalmic artery aneurysm (*arrow*), its neck, and the ICA.

on 3-D CT angiograms than on conventional angiograms. Aneurysms adjacent to bone may not be clearly depicted on 3-D CT angiograms owing to the limitation of the threshold CT value. Therefore, 3-D CT angiography is less useful than conventional angiography for depicting intracranial aneurysms adjacent to bone. In our study, 17 (63%) of 27 ICA aneurysms were not clearly delineated on 3-D CT angiograms. The subtraction 3-D CT angiograms clearly showed these 17 ICA aneurysms and the surrounding vascular structures noninvasively and was superior or equivalent to conventional angiography in depicting these aneurysms. Therefore, we believe that subtraction 3-D CT angiography is useful for delineating intracranial aneurysms adjacent to bone. The need to exclude bone structures manually on the axial images in order to depict aneurysms and the surrounding structures at the skull base has been noted in a previous study (7). In that report, CT angiograms of aneurysms at the skull base were inadequate owing to the limitations of manual subtraction techniques, and they were inferior to magnetic resonance (MR) angiograms and conventional angiograms in depicting aneurysms at the skull base (7). Furthermore, those CT angiograms were maximum-intensity projection images and were inferior to 3-D CT angiograms.

Görzer et al (10) reported the use of spiral CT angiography with digital subtraction techniques. These authors used a stereotactic frame or an atraumatic fixation system for decreasing motion artifacts. Fixation is important for obtaining a good subtraction 3-D CT angiogram. Another technical consideration is the synchronization of the table movement and X-ray tube rotation before and after administration of contrast medium. Our subtraction processing technique with the newly devised controlled-orbit helical scanning is a valuable method by which to obtain good subtraction 3-D CT angiograms. With the use of subtraction 3-D CT angiography together with 3-D CT angiography, we were able to depict precisely all intracranial aneurysms. We hope that this success will decrease the number of conventional angiograms needed.

We did not compare 3-D CT angiography with MR angiography. Although MR angiography is a useful screening method, because it can be obtained without contrast administration (11–15), it has the disadvantage of producing flow-related artifacts and causing image degradation from motion artifacts (16).

Conclusion

Three-dimensional CT angiography with helical scanning is a useful method for delineating intracranial aneurysms. Our technique, subtraction 3-D CT angiography with controlled-orbit helical scanning, was useful for the detection of aneurysms adjacent to bone.

References

1. Schmid UD, Steiger HJ, Huber P. **Accuracy of high resolution computed tomography in direct diagnosis of cerebral aneurysms.** *Neuroradiology* 1987;29:152–159
2. Newell DW, LeRoux PD, Dacey RG Jr, et al. **CT infusion scanning for the detection of cerebral aneurysms.** *J Neurosurg* 1989;71:175–179
3. Aoki S, Sasaki Y, Machida T, et al. **Cerebral aneurysms: detection and delineation using 3D CT angiography.** *AJNR Am J Neuroradiol* 1992;13:1115–1120
4. Hope JKA, Wilson JL, Thomson FJ. **Three-dimensional CT angiography in the detection and characterization of intracranial berry aneurysms.** *AJNR Am J Neuroradiol* 1996;17:439–445
5. Ogawa T, Okudera T, Noguchi K, et al. **Cerebral aneurysms: evaluation with three-dimensional CT angiography.** *AJNR Am J Neuroradiol* 1996;17:447–454
6. Dillon EH, van Leeuwen MS, Arancha Fernandez M, et al. **Spiral CT angiography.** *AJR Am J Roentgenol* 1993;160:1273–1278
7. Schwartz RB, Tice HM, Hooten SM, et al. **Evaluation of cerebral aneurysms with helical CT: correlation with conventional angiography and MR angiography.** *Radiology* 1994;192:717–722
8. Vieco PT, Shuman WP, Alsofrom GF, et al. **Detection of circle of Willis aneurysms in patients with acute subarachnoid hemorrhage: a comparison of CT angiography and digital subtraction angiography.** *AJR Am J Roentgenol* 1995;165:425–430
9. Alberico RA, Patel M, Casey S, et al. **Evaluation of the circle of Willis with three-dimensional CT angiography in patients with suspected intracranial aneurysms.** *AJNR Am J Neuroradiol* 1995;16:1571–1578
10. Görzer H, Heimberger K, Schindler E. **Spiral CT angiography with digital subtraction of extra- and intracranial vessels.** *J Comput Assist Tomogr* 1994;18:839–841
11. Curnes JT, Shogry MEC, Clark DC, et al. **MR angiographic demonstration of an intracranial aneurysm not seen on conventional angiography.** *AJNR Am J Neuroradiol* 1993;14:971–973
12. Gouliamos A, Gotsis E, Vlahos L, et al. **Magnetic resonance angiography compared to intra-arterial digital subtraction angiography in patients with subarachnoid hemorrhage.** *Neuroradiology* 1992;35:46–49
13. Schnierer G, Huk NJ, Laub G. **Magnetic resonance angiography of intracranial aneurysms: comparison with intra-arterial digital subtraction angiography.** *Neuroradiology* 1992;35:50–54
14. Heinz RE. **Aneurysms and MR angiography.** *AJNR Am J Neuroradiol* 1993;14:974–977
15. Ross JS, Masaryk TJ, Modic MT, et al. **Intracranial aneurysms: evaluation by MR angiography.** *AJNR Am J Neuroradiol* 1990;11:449–456
16. Masaryk TJ, Modic MT, Ross JS, et al. **Intracranial circulation: preliminary results with three-dimensional (volume) MR angiography.** *Radiology* 1989;171:793–799